Moisture-dependent Water Repellency of Greenlandic Cultivated Soils

Weber, Peter L.; Hermansen, Cecilie; Norgaard, Trine; Pesch, Charles; Moldrup, Per; Greve, Mogens H.; Müller, Karin; Arthur, Emmanuel; de Jonge, Lis Wollesen

Published in:
Geoderma

DOI (link to publication from Publisher):
10.1016/j.geoderma.2021.115189

Publication date:
2021

Document Version
Publisher's PDF, also known as Version of record

Geoderma 402 (2021) 115189

Contents lists available at ScienceDirect

Geoderma

journal homepage: www.elsevier.com/locate/geoderma

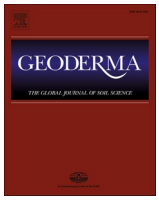

Moisture-dependent Water Repellency of Greenlandic Cultivated Soils

Peter L. Weber [a,*], Cecilie Hermansen [a], Trine Norgaard [a], Charles Pesch [b], Per Moldrup [b], Mogens H. Greve [a], Karin Müller [c], Emmanuel Arthur [a], Lis Wollesen de Jonge [a]

[a] Dept. of Agroecology, Faculty of Technical Sciences, Aarhus University, Blichers Allé 20, DK-8830 Tjele, Denmark
[b] Dept. of the Built Environment, Faculty of Engineering and Science, Aalborg University, Thomas Manns Vej 23, DK-9220 Aalborg Ø, Denmark
[c] The New Zealand Institute for Plant & Food Research Limited (PFR), Land Use Impacts, Private Bag 3230, Waikato Mail Centre, Hamilton 3240, New Zealand

ARTICLE INFO

Handling Editor: Morgan Cristine L.S.

Keywords:
Soil water repellency
Subarctic agriculture
Molarity of an ethanol droplet
Loss-on-ignition
Soil water retention
Greenland
New Zealand

ABSTRACT

The rapid warming of the Arctic is changing the conditions for agricultural activity in southwest Greenland markedly, which necessitates studies of the physical properties of the soil resource. Soil water repellency (SWR) is a soil property that changes soil functional behaviour across a soil-specific range in water-content (W). Although SWR occurs worldwide, it has not been studied in sub-arctic pasture and grass fields. Thus, the aim was to examine the prevalence of SWR in South Greenland and to establish pedotransfer functions for SWR on soil properties that are faster to measure than SWR, i.e. soil organic fractions, texture and soil water retention. This study included 145 soil samples from 22 sub-arctic agricultural fields distributed across three areas of South Greenland, with broad distributions in texture (clay: 0.017–0.194 kg kg^{-1}) and organic carbon (OC) (0.009–0.241 kg kg^{-1}) contents. The degree of soil water repellency (SWR) as a function of water content (SWR-W curve) was measured from oven-dry conditions to the water-content at which the soil became hydrophilic (W_{NON}), and total SWR (SWR_{AREA}) was calculated as the integrated trapezoidal area (SWR_{AREA}) of the SWR-W curve. A total of 99% and 98% of the soil samples were water-repellent and extremely water repellent at their maximum SWR, respectively. Among the three soil organic fractions (OC, Loss-on-ignition at 550 °C, and 225 °C (LOI_{550} and LOI_{225})), LOI_{550} was the best predictor of SWR_{AREA} and W_{NON} (both with $r^2 = 0.93$). Multiple linear regressions including clay content increased r^2_{adj} to 0.92 and 0.95 with OC and LOI_{550}, respectively. The Campbell-Shiozawa (CS) model was fitted to the soil–water retention curves (pF 3.0–6.9), and the inverse slope ($-\alpha^{-1}$) of the CS model exhibited a high correlation to both SWR_{AREA} (r^2_{adj} of 0.87) and W_{NON} (r^2_{adj} of 0.93), thus suggesting that soil water retention governs SWR. Lastly, it was shown that the coefficient of proportionality between OC and both SWR_{AREA} and W_{NON} for these sub-arctic soils coincided with pasture soils from New Zealand.

1. Introduction

Climate change is particularly pronounced in the Arctic region, which is warming at twice the global average rate (Francis and Vavrus, 2012). The warming climate has severe repercussions for the Arctic ecosystems, which poses a threat to the traditional livelihoods of the indigenous Arctic peoples (Nuttall, 2018). The warming climate does, however, expand the northern boundary for agricultural activity (King et al., 2018), which presents an opportunity for increased agricultural production in e.g. southwest Greenland (Christensen et al., 2016; Westergaard-Nielsen et al., 2015). Climate simulations predict that the current duration of the growing season will extend by approximately two months at the end of this century (Christensen et al., 2016). The changing climate necessitates an adaptation of the farming practices, and knowledge of the agricultural soil resource is needed to underpin future adaptation strategies (Caviezel et al., 2017).

Only a few studies have investigated the Greenlandic agricultural soils. The soils have generally been characterized by being acidic, highly organic, and coarsely textured (Caviezel et al., 2017; Ogrič et al., 2019; Pesch et al., 2020; Weber et al., 2020), which is a combination that has

Abbreviations: LOI_{225}, Loss-on-ignition after 225 °C; LOI_{550}, Loss-on-ignition after 550 °C; MLR, Multiple linear regression; OC, Organic carbon; OM, Organic matter; SSA, Specific surface area; SWR, Soil water repellency; SWR_{AREA}, Trapezoidal integrated area under the SWR-W curve; SWRC, Soil water retention curve; W, Gravimetric water content; W_{NON}, Critical water content; $-\alpha^{-1}$, The inverse of the Campbell Shiozawa slope.

* Corresponding author.
E-mail address: plw@agro.au.dk (P.L. Weber).

https://doi.org/10.1016/j.geoderma.2021.115189
Received 23 September 2020; Received in revised form 16 April 2021; Accepted 28 April 2021
Available online 21 May 2021

been shown to induce soil water repellency (SWR) under dry conditions (de Jonge et al., 1999; Doerr et al., 2000; Hermansen et al., 2019). Soil water repellency (SWR) is a functional soil property that has been investigated worldwide across different geographic and climatic regions (Doerr et al., 2005b, 2000; Regalado et al., 2008), and some SWR surveys found a high prevalence of SWR across large datasets (Deurer et al., 2011; Hermansen et al., 2019; Seaton et al., 2019). Despite the ubiquity of SWR, it has not been studied in sub-arctic grass and pasture soils, which include the vast majority of the agricultural area in SW Greenland (Westergaard-Nielsen et al., 2015). Additionally, the growing seasons are often very dry (Caviezel et al., 2017) and the frequency and duration of dry periods are similarly forecasted to increase (Christensen et al., 2016), which may further increase the SWR.

Soil organic matter (OM) can form hydrophobic coatings on soil particles and aggregates (Bisdom et al., 1993; Capriel et al., 1990; Giovannini et al., 1983). Some implications of SWR can be finger flow (Dekker and Ritsema, 1995), reduced infiltration rate, and increased overland flow (Doerr et al., 2000; Leighton-Boyce et al., 2007). The consequences of SWR can be negative with respect to, e.g., reduced crop productivity and irrigation efficiency (Müller et al., 2010) and increased leaching risk of agrochemicals to groundwater (Dekker and Ritsema, 1995). However, SWR can also serve as an adaptive stress response, which may be an indicator of an ecosystems resilience towards environmental stressors such as drought (Seaton et al., 2019).

Since SWR is a transient soil property (Graber et al., 2009), the soil is only resistant towards wetting across a soil-specific range in water content (W). Some soils are hydrophobic already from zero W at oven-dried conditions (105 °C), whereas other soils first become hydrophobic at a W around or above air-dry conditions. The shape of the SWR versus W (SWR-W) curve mainly falls within three overall categories; flat curves (hydrophilic soils), single-peak curves, and double-peak curves (de Jonge et al., 1999; Hermansen et al., 2019; Regalado et al., 2008). For the single-and double peak curves, SWR varies nonlinearly with W, and the critical water content (W_{NON}) constitutes the W above which the soil remains hydrophilic (Dekker and Ritsema, 1994, 1995; Wijewardana et al., 2016).

Measuring SWR-W curves is very time-consuming. However, SWR parameters such as the integrated trapezoidal area of the SWR-W curve (SWR_{AREA}) and W_{NON} may be derived from easily measurable soil properties (Regalado et al., 2008). Furthermore, the SWR_{AREA} and W_{NON} constitute key parameters for characterizing the SWR-W curve because they denote the total severity in SWR of a soil sample across all moisture contents and the W at which SWR ceases, respectively. The OC content is the primary physiochemical soil property controlling the severity of SWR (Hermansen et al., 2019; Seaton et al., 2019). Thus, it is consistent throughout the literature that SWR_{AREA} and W_{NON} increase with increasing OC content (de Jonge et al., 1999, 2007; Hermansen et al., 2019; Regalado and Ritter, 2005). Although it is well studied how SWR_{AREA} and W_{NON} correlate to OC, it has not yet been reported whether OM, measured by loss-on-ignition (LOI) (Hoogsteen et al., 2015) at 550 °C (LOI_{550}), could provide a better estimate of these SWR parameters. Heat treatments with LOI at varying temperatures affect the severity of SWR (Wu et al., 2020). For example, it has been shown that SWR can increase when the soil is exposed to high temperatures for short durations (e.g., up to 300 °C for 20 to 60 min (Doerr et al., 2005a)), and ultimately can be eliminated when the soil is exposed to heating for more extended time periods (e.g., 225 °C for 5 h (Simkovic et al., 2008)). In the study of Simkovic et al. (2008), heating at 225 °C for 5 h changed OM quality, and the most significant finding was that aliphatic structures were thermally degraded, which might be the explanation for the elimination of SWR. Assuming the degradation of aliphatic SOM structures is proportional to the mass-loss after LOI at 225 °C (LOI_{225}), it is intriguing if LOI_{225} possesses a higher correlation to SWR_{AREA} and W_{NON} as compared to LOI_{550} at which all OM is removed (Hoogsteen et al., 2015).

Concerning the effect of texture on SWR, water repellency occurs in both fine- and coarse-textured soils (Bisdom et al., 1993; Dekker and Ritsema, 1996; Doerr et al., 2000). With regard to clay content, some studies found that clay content affected the variation in SWR_{AREA} insignificantly (de Jonge et al., 1999; Hermansen et al., 2019; Karunarathna et al., 2010b). Contrarily, the clay-to-OC ratio might affect SWR. The Dexter *n* clay saturation index (Dexter et al., 2008), which denotes that 8–10 g of clay can complex an upper limit of 1 g of OC, was useful to distinguish between water repellent and wettable soils in the study of Karunarathna et al. (2010b). In the study of Karunarathna et al. (2010b) water repellent soils exhibited a clay-to-OC ratio above 8.

As compared to measuring the entire SWR-W curve, it is faster to measure the soil–water retention curve (SWRC) between pF 6.9 and 3.0 using, for example, a chilled-mirror WP4-T dewpoint potentiometer (Decagon Devices Inc., Pullman, WA). The semi-logarithmic Campbell-Shiozawa (CS) function (Campbell and Shiozawa, 1992) relates the soil water matric potential to soil water content in the dry end of the SWRC (Pittaki-Chrysodonta et al., 2019). The inverse slope of this CS function ($-\alpha^{-1}$) correlates linearly to OM and clay contents (Pittaki-Chrysodonta et al., 2019). Thus, it is interesting to investigate if the $-\alpha$ parameter can serve as a link between the SWRC and the SWR-W curve.

With the emerging opportunities for future agricultural productions in Greenland, there is a need to assess the distribution and severity of SWR of sub-arctic grass and pasture soils. Thus, it would be advantageous if SWR_{AREA} and W_{NON} could be derived from pedotransfer functions based on soil properties that are faster to measure. For a dataset consisting of soil samples collected from sub-arctic grass and pasture fields, the aims were to assess:

i) The frequency and severity of SWR,
ii) The correlation between SWR parameters (SWR_{AREA} and W_{NON}) and parameters characterizing soil organic fractions (OC, LOI_{225}, and LOI_{550}),
iii) The impact of texture and Dexter *n* (clay-to-OC saturation index) on SWR,
iv) Whether soil water retention (the inverse slope of the Campbell-Shiozawa (CS) model (pF3.0 to 6.9)), can predict SWR_{AREA} and W_{NON},
v) If OC controls SWR across datasets of varying geographic and climatic regions (combined dataset with soils from Greenland and New Zealand).

2. Materials and methods

2.1. Study sites

The study comprised 145 soil samples distributed across 23 pasture and cultivated fields, which are located within the Tunulliarfik and Igalikup Kangerlua fjord systems in south Greenland (Fig. 1). The majority of the fields were located within the agricultural regions of Qassiarsuk (QA, 61°09′N 45°30′W), Igaliku (IG, 61°00′N 45°26′W), and South Igaliku (SI, 60°53′N 45°16′W), which cover three of the main agricultural areas in Greenland (Westergaard-Nielsen et al., 2015). Additionally, one field was sampled at the research station in Upernaviarsuk (60°44′57.3″N 45°53′24.4″W). This was grouped with the IG soils for the sake of simplicity. This division into three regions roughly mirrors the differences in the parent material in the region with basalt and sandstone of the Eriksfjord formation (QA), granitic Julianehåb batholith (IG and SI), and sandy aeolian loess (SI) (Jacobsen, 1987; Steenfelt et al., 2016).

The broader study area occupies the ice-free area between the Greenland ice sheet and the Labrador Sea, which is characterized by its mountainous landscape that is bisected by numerous glacial fjords. While a large part of the mountainous landscape is used as pasture for sheep grazing, the cultivated area is primarily interspersed throughout places that offer adequate soil moisture, favourable microclimates, and the immediate vicinity of the fjords (Caviezel et al., 2017; Westergaard-

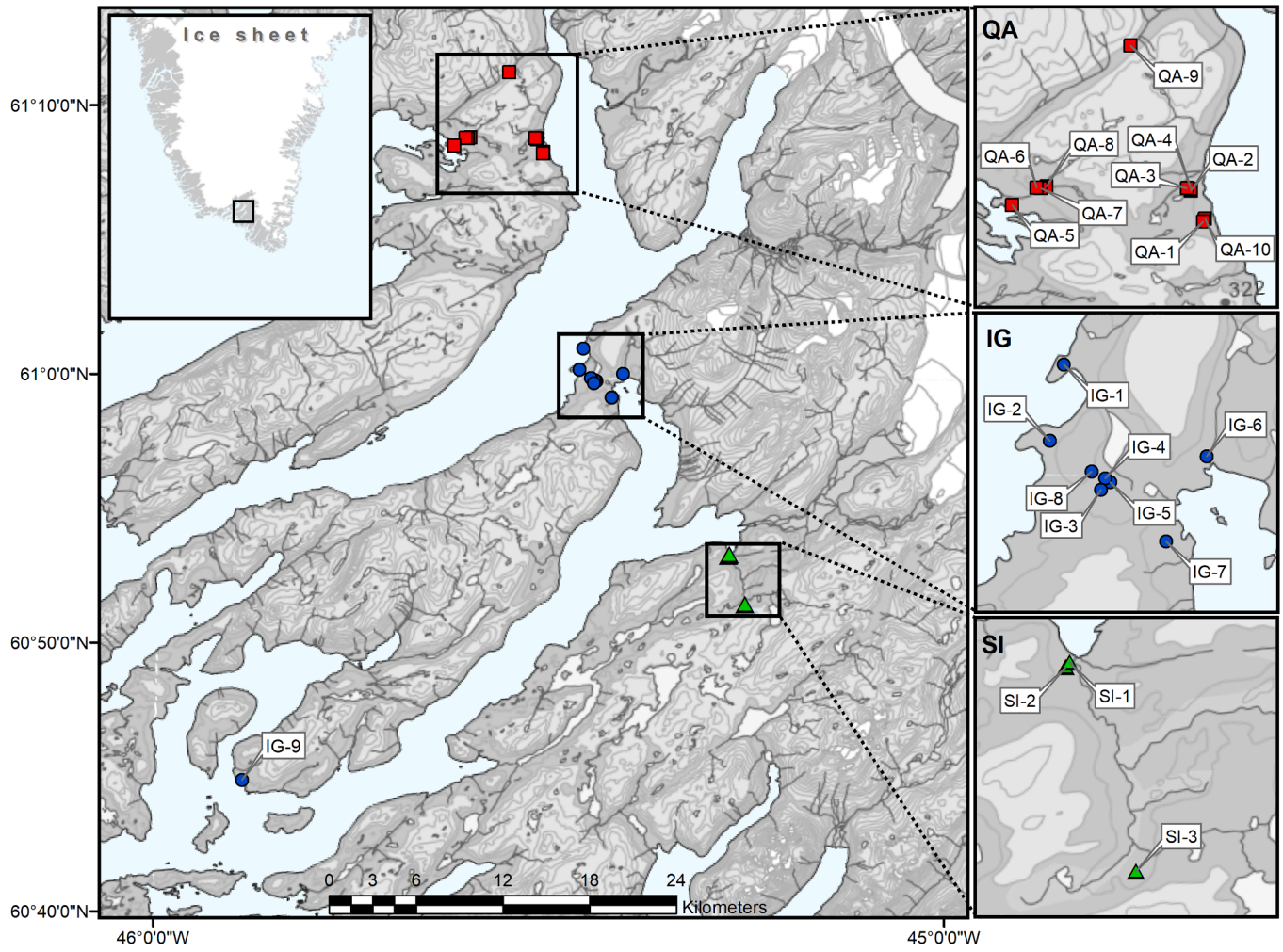

Fig. 1. Location of the 22 investigated fields across the three main areas Qassiarsuk (QA), Igaliku (IG), and Sdr. Igaliku (SI).

Nielsen et al., 2015). The study area coincides with the newly appointed UNESCO world heritage site "Kujataa," which serves to protect the agricultural activity and its history, which dates as far back as the Norse Landnám c.a. 985 CE. In the inner part of the fjords, the climate is subarctic with a mean temperature in July of 10.3 °C (Hanna and Cappelen, 2002), and the study area is situated south of the discontinuous permafrost zone (Daanen et al., 2011). The mean annual temperature and precipitation range from 0.6 °C to 0.9 °C and 615 mm to 858 mm, respectively, depending on the vicinity to the ocean (Hanna and Cappelen, 2002).

The investigated fields were used for hay production, with the exception of IG-6, SI-1, and SI-2, which were abandoned and solely used for grazing. The extent of the field varied between 1 and 12 ha. The vegetation of the areas used for hay typically comprised grass mixtures consisting of, e.g., colonial bentgrass (*Agrostis tenuis* L.), Kentucky bluegrass (*Poa pratensis* L.), Perennial ryegrass (*Lolium perenne* L.), red fescue (*Festuca rubra* L.), and timothy (*Phleum pratense* L.). Wild unsown grass species were also present in some of the investigated fields, especially the three pasture fields, and IG-6 also included small patches of greyleaf willow (*Salix glauca* L.) and dwarf birch (*Betula nana* L.).

2.2. Soil sampling and analysis

Soil samples were collected during three sampling campaigns in 2015, 2017, and 2018, which all took place in August. >550 soil samples were initially acquired in rectangular grids with 7.5- by 7.5-m to 15- by 15-m spacing. However, the present study was limited to a subset of 145 soil samples due to the cumbersome nature of soil water repellency measurements. The subset of 145 soil samples was carefully selected by including 1 to 13 samples from each field to cover the largest variation in OC and clay within each field and across the textural classes. Additionally, two large representative fields (IG-1 and IG-2) were included in the dataset.

Approximately 2 kg of bulk soil was sampled from the upper 5 cm of the A-horizon directly below the turf, which corresponded to a maximum soil depth of approximately 5–15 cm. Prior to all analyses, the bulk soil was air-dried in a well-ventilated laboratory at 20 °C and subsequently dry-sieved to < 2 mm. The soil pH was determined in a soil/water suspension of 1:4 (v/v), and soil texture was determined after removal of SOM by a combination of wet-sieving and the pipette method (Gee and Or, 2002). None of the investigated soils tested positive for calcium carbonate with 10% hydrochloric acid; thus OC was directly determined by high-temperature dry combustion using an ELTRA Helios C-Analyzer (ELTRA GmbH, Haan, NW, Germany).

Loss-on-ignition was determined at both 225 °C (LOI_{225}) and 550 °C (LOI_{550}). Six grams of air-dry soil was added to clean and pre-ignited crucibles, and oven-dry soil weight was determined after oven-drying at 105 °C for 24 h in a ventilated oven. The crucibles were subsequently stepwise ignited at 225 °C and 550 °C for 12 h in a half-full Nabertherm L 40/11 muffle furnace (Nabertherm GmbH, Lilienthal, NI, Germany) to ensure an even ignition. Samples were cooled to room temperature in a desiccator and weighed between each heat treatment, and LOI_{225} and LOI_{550} were expressed as the mass losses per unit of oven-dry soil (Hoogsteen et al., 2015). Finally, SOM was calculated from

OC using a OC/SOM ratio of 2.0 (Pribyl, 2010), which agreed well with the OC/LOI_{550} ratio for the investigated soils (Fig. A1).

2.3. Soil water repellency

The soil water repellency (SWR) was determined with the molarity ethanol droplet (MED) test (de Jonge et al., 1999; King, 1981; Roy and McGill, 2002), using the same approach as Hermansen et al. (2019). Briefly, the soil samples were quickly placed in plastic containers, and a uniform sample surface was ensured by leveling the surface and subjecting it to a normal stress of 60.9 Nm^{-2} for two minutes. A series of ethanol and deionized solutions were made for ethanol concentrations between 0.00 and 0.80 $m^3\ m^{-3}$ in concentration increments of 0.01 $m^3\ m^{-3}$. A 60 µL droplet of ethanol solution was then carefully placed on the surface of a soil sample and left to infiltrate for five seconds. The highest ethanol concentration that did not infiltrate the soil within five seconds was then used to calculate the surface tension of the soil sample following Roy and McGill (2002). This procedure was then performed on soil samples, which had been pretreated to reach varying gravimetric water contents (W), resulting in the full SWR-W curve (Fig. 2). The pretreatments included 48 h equilibration in a 20 °C climate-controlled laboratory (SWR_{AD}), oven-drying at 60 °C for 24 h immediately followed by a 48 h equilibration in the same laboratory (SWR_{60}), and oven-drying at 105 °C for 24 h followed by cooling in a desiccator for 2 h (SWR_{105}).

Additionally, pretreatments for specific W were made by thoroughly mixing tap water and air-dried soil in small plastic bags and equilibrating them in a dark fridge at 4 °C for a minimum of two weeks. The increments in W were based on the expected W_{NON}, which was calculated using the linear regression between W_{NON} and OC reported by Hermansen et al. (2019) for 72 New Zealand pasture soils (see Fig. 10). The final increments in W ranged between 0.002 and 0.171 kg kg^{-1}, and the actual W of the soil samples were determined by oven-drying a subsample of the pretreated soil samples. The integrated trapezoidal area under the SWR-W curve was used to evaluate the total degree of SWR, and the W_{NON} was determined as the highest water content where the soil remains hydrophobic (Fig. 2).

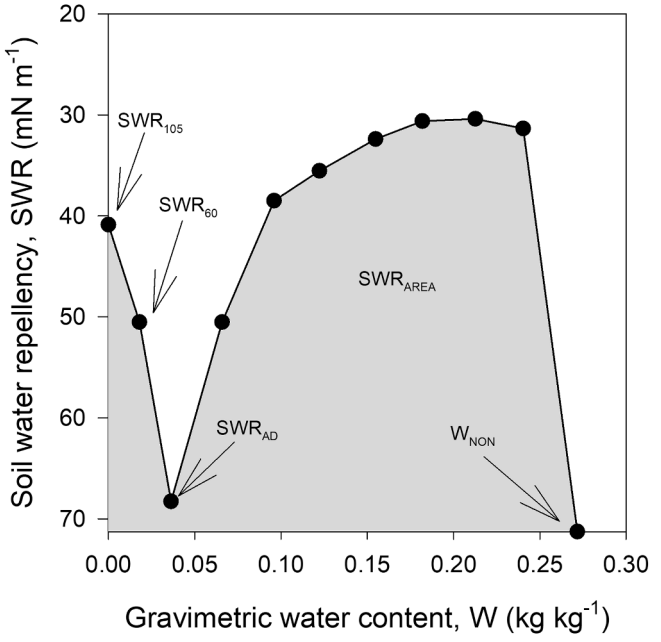

Fig. 2. Conceptual illustration of the integrated trapezoidal area (SWR_{AREA}) of the SWR-W curve and the critical soil–water content (W_{NON}). SWR_{105}, SWR_{60}, and SWR_{AD} denote the standardized pretreatments where the soil is dried at 105 °C, 60 °C, and air-dried conditions, respectively. Note the inverted y-axis, as SWR is inversely related to surface tension (after Hermansen et al., 2019).

2.4. Soil water retention

With the exception of the oven-dried soils, the soil matric potential was determined on a subsample of the pretreatments using a chilled-mirror WP4-T Dewpoint Potentiometer (Decagon Devices Inc., Pullman, WA, USA), which is capable of measuring matric potentials between pF 3 and pF 6.5. Matric potentials (ψ) were expressed as pF following Schofield (1935), where $pF = \log_{10}(|\psi, \text{cm } H_2O|)$, and matric potential at oven-dry was set to pF 6.9 (Groenevelt and Grant, 2004). The semi-logarithmic Campbell-Shiozawa (CS) function (Campbell and Shiozawa, 1992) was used as a simple model for the soil water retention in the dry region between pF 6.9 and pF 3.0:

$$pF = pF_0 - \alpha W \quad (1)$$

where W is the gravimetric water content (kg kg^{-1}), α is the dimensionless slope of the log-linear $\log_{10}(|\psi, \text{cm } H_2O|)$-W relationship, and pF_0 is the intercept, i.e., the pF under oven-dry conditions. The simple CS model was subsequently used to normalize the SWR to pF rather than W, which enabled a direct comparison of SWR-curves between pF 6.9 and pF 3.0, regardless of the soil water retention characteristics.

2.5. Statistical analysis

Linear correlations were evaluated by the coefficient of determination (r^2). Forward multiple linear regressions (MLRs) were used to correlate physicochemical properties (clay, silt, sand, OC, and pH), heat treatments (LOI_{225} and LOI_{550}), and soil water retention ($-\alpha^{-1}$) to SWR_{AREA} and W_{NON}. The MLRs were performed in Sigma Plot 11.0 (Systat Software, Inc.), and only soil properties that contributed significantly ($p < 0.5$) were used in the final MLRs of W_{NON}.

3. Results and discussion

3.1. Physiochemical soil properties

The 145 soil samples collected across the areas of Qassiarsuk, Igaliku, and South Igaliku, altogether spanned four soil textural classes (sand, loamy sand, sandy loam, and loam) within the USDA soil textural

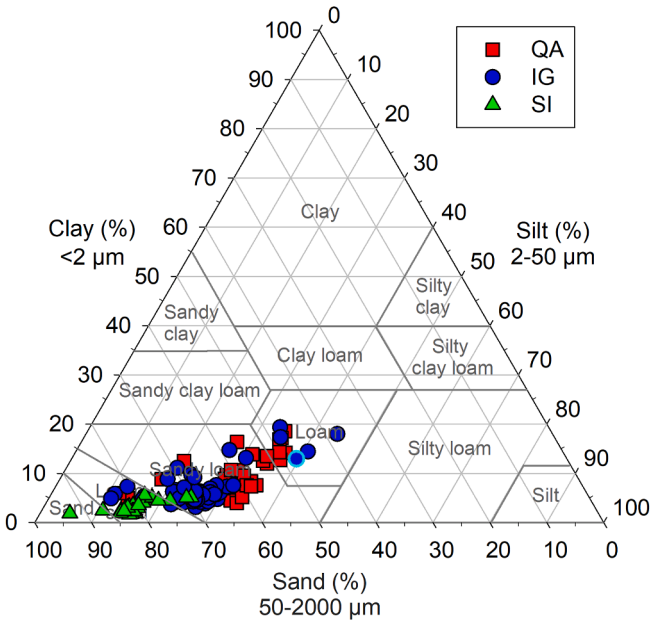

Fig. 3. Distribution of the 145 investigated soil samples within the USDA texture triangle. The single hydrophilic soil from Igaliku is marked with a cyan border.

triangle (Fig. 3). The soil samples from South Igaliku represented the group of soil samples with the coarsest texture (sand to sandy loam), although there was some overlap to the soil samples from Igaliku and Qassiarsuk (loamy sand to loam). Only one of the investigated soil samples was hydrophilic, and the 144 water repellent soil samples exhibited clay and OC contents from 0.017 to 0.194 kg kg^{-1} and 0.009 to 0.241 kg kg^{-1}, respectively. The LOI_{225} and LOI_{550} contents ranged from 0.017 to 0.527 kg kg^{-1} and 0.026 to 0.609 kg kg^{-1}, respectively. Further, the samples represented acidic to neutral soils with pH ranging from 4.5 to 7.5.

3.2. Frequency and severity of SWR in Greenlandic soils

Within this study, 99% of the soils were water repellent at some W (144 out of 145 samples). It was suggested by Doerr et al. (2000), that samples exhibiting surface tensions $\leq$ 40.88 mN m^{-1} are extremely hydrophobic. According to this definition, 98% of the soil samples exhibited an extreme degree of hydrophobicity (142 out of 145 samples) (Fig. 4). Other studies also found a high prevalence of SWR. An SWR survey on soils collected under pastoral land use across the North Island of New Zealand found that 98% of the studied sites (49 out of 50 sites) could potentially become water repellent upon drying (Deurer et al., 2011). Another study by Hermansen et al., 2019 on pastoral soils from the South Island of New Zealand found that 92% of the samples were water repellent (72 out of 78 samples). Lastly, a survey across different habitats in Wales (bog, forest, arable, and grassland) found 68% of the soils to exhibit moderate to extreme SWR and 92% of the soils to exhibit some SWR (Seaton et al., 2019).

It is evident from Fig. 4 that this dataset represents the wide variety of SWR-W curve shapes published in the literature (de Jonge et al., 1999, 2007; Karunarathna et al., 2010a; Regalado and Ritter, 2009; Regalado et al., 2008). The dataset includes hydrophilic (data not shown), unimodal (Fig. 4i), and bimodal (Fig. 4a) SWR-W curves. For the unimodal curves, it was most common for this dataset, that the soils were hydrophilic at zero W, meaning that the onset of SWR occurred at a W around or above-air-dried conditions. Thus, many of these soils exhibiting unimodal behaviour would have been classified as hydrophilic if SWR measurements had been performed only on oven-dried and air-dried samples. The soils exhibiting bimodal behaviour were water repellent at zero W, with a drop in SWR around air-dry W. At this point, the SWR decreased to a lower degree of SWR or hydrophilic conditions, which is consistent with findings in other studies (de Jonge et al., 1999; Regalado et al., 2008). Within each field, some SWR-W curves were exclusively unimodal (e.g., Fig. 4, QA-10), bimodal (e.g., Fig. 4, IG-1) or a combination of the two (e.g., Fig. 4, QA-6).

The SWR_{AREA} and W_{NON} were highly variable, ranging from 0.54 to 25.89 mN m^{-1} and 0.052 to 0.921 kg kg^{-1}, respectively (Table 1). Among the three main areas, the soils from South Igaliku had the lowest mean SWR_{AREA} (2.70 mN m^{-1}) as compared to the soils from Igaliku and Qassiarsuk, which had mean SWR_{AREA} values of 6.06 and 9.58 mN m^{-1}. The same trend was valid for W_{NON}. The total range for W_{NON} was 0.052 to 0.921 kg kg^{-1}, and the mean values for the three areas were 0.104, 0.221, and 0.355 kg kg^{-1} for South Igaliku, Igaliku, and Qassiarsuk, respectively. Thus, the soils from South Igaliku (Fig. 4r–t) were water repellent within a relatively narrow range in W, as compared to the soils from Qassiarsuk and Igaliku (Fig. 4a–q).

Some fields (e.g., Fig. 4a, f, and h) represented a high range in SWR_{AREA} and W_{NON}. For example, field QA-1 (Fig. 4a) had SWR_{AREA} values between 3.562 and 25.893 mN m^{-1} and W_{NON} values between 0.164 and 0.921 kg kg^{-1}. The soils exhibiting the lowest and highest OC contents of this field (0.042 and 0.241 kg kg^{-1}) were simultaneously the soils with the lowest and highest SWR_{AREA}. Within the remaining fields, the soil samples having the lowest and highest SWR_{AREA} also had correspondingly low and high OC contents (Fig. 4), indicating a strong influence from OC on the severity in SWR.

The investigated soil samples exhibited a strong linear relationship between pF and gravimetric water content between pF 6.9 and pF 3.0 (Fig. 5a), and the CS-model adequately described the dry-region SWRC of the soils with an $r^2 > 0.95$ for all but one sample. The CS-slope, α, increased nonlinearly with OC content and the inverse of the CS-slope, $-\alpha^{-1}$, was positively correlated with clay content ($r = 0.61$) and strongly linearly correlated with OC ($r = 0.93$). Previous studies on water-sorption isotherms have shown that $-\alpha^{-1}$ is proportional to the soil specific surface area (SSA) (Arthur et al., 2013; Resurreccion et al., 2011). Assuming that $-\alpha^{-1}$ is also proportional to SSA in this study, the strong linear relationship between $-\alpha^{-1}$ and OC indicates that SOM is the principal parameter governing the SSA and dry-region SWRC ($-\alpha^{-1}$) of these Greenlandic soils.

The fitted CS-models were subsequently used to convert W to pF for the SWR-pF curves, which enabled a direct comparison of the SWR-curves between pF 6.9 and pF 3.0 (Fig. 5b). The SWR-pF curves revealed a remarkable similarity in the shape of the peak that occurs at water contents higher than air-dry, which started in the pF range between 6 and 5 (shown for three representative soils in Fig. 5b). It was common for the soil samples to exhibit an extreme degree of SWR (<40.88 mN m^{-1}) (Doerr et al., 2000) at the permanent wilting point (WP; pF = 4.2), with further increases in SWR after WP for the more organic soils (Fig. 5b). Further, the W_{NON} occurred at a pF < 3. The ability of the SWR-pF curve to normalize the shape of the SWR peaks across soil textural classes has previously been reported by, e.g. Karunarathna et al. (2010b) and Wijewardana et al. (2016). Further, Regalado et al. (2008) reported similar SWR-pF curves for a diverse dataset, which included subtropical volcanic soils (Kawamoto et al., 2007; Regalado and Ritter, 2005), temperate mineral soils (de Jonge et al., 2007; King, 1981), and a set of Icelandic Andosols and Histosols (Bartoli et al., 2007). Regalado et al. (2008) similarly found that SWR increased rapidly from air-dry (app. pF 6) towards the maximum SWR (approx. pF 4.2) and that hydrophobicity occurred around pF 2.5. The similarity of the SWR-pF curves between the Greenlandic soils and the findings of Regalado et al. (2008) is remarkable, as it indicates a somewhat universal SWR-pF behaviour of extremely varied soils. The similar behavior of the SWR-pF curves may be due to a pF-dependent reorientation of the functional groups of the SOM, where the hydrophobic functional groups are orientated outwards around the SWR maxima (Doerr et al., 2000). It should, however, be stressed that the normalization of the SWR-pF curve is limited to the location of the peaks on the pF-axis, as the severity of SWR at a given pF increases with OC content (Fig. 5b).

3.3. Correlations between SWR and soil organic fractions

Linear regressions for SWR_{AREA} and W_{NON} based on OC revealed a high linear correlation between both parameters (SWR_{AREA} and W_{NON}) and OC content ($r^2 = 0.91$ and 0.88, respectively) (Fig. 6a and d). Other studies also found linear correlations between SWR_{AREA} and OC or OM. Regalado et al. (2008) included soils from Australia, Iceland, Denmark, Japan, and Spain in a linear regression for SWR_{AREA} using OM as a predictor variable and obtained an r^2 of 0.82. Similarly, the study of Regalado and Ritter (2005) reported a linear regression ($r^2 = 0.60$) between SWR_{AREA} and OC for Spanish soils. Further, the study of de Jonge et al. (1999) reported a linear correlation ($r = 0.79$) between SWR_{AREA} and OC for 14 Danish soil samples. However, not all studies reported linear correlations. A Langmuir-type model utilizing OC to determine SWR_{AREA} was also suggested (Wijewardana et al., 2016). Similar to SWR_{AREA}, a linear correlation between W_{NON} and OC has been found in several studies. For example, de Jonge et al. (2007) found a linear correlation ($r = 0.80$) between W_{NON} and OC for soil samples from Denmark, and Kawamoto et al. (2007) developed a linear regression for W_{NON} based on OC yielding an r^2 of 0.76.

Substantial heating of soil samples to 225 °C for a duration of 5 h (Simkovic et al., 2008) or 14–20 h for peat soils (Wu et al., 2020) can eliminate SWR. During heating to 225 °C for extended time periods, OM

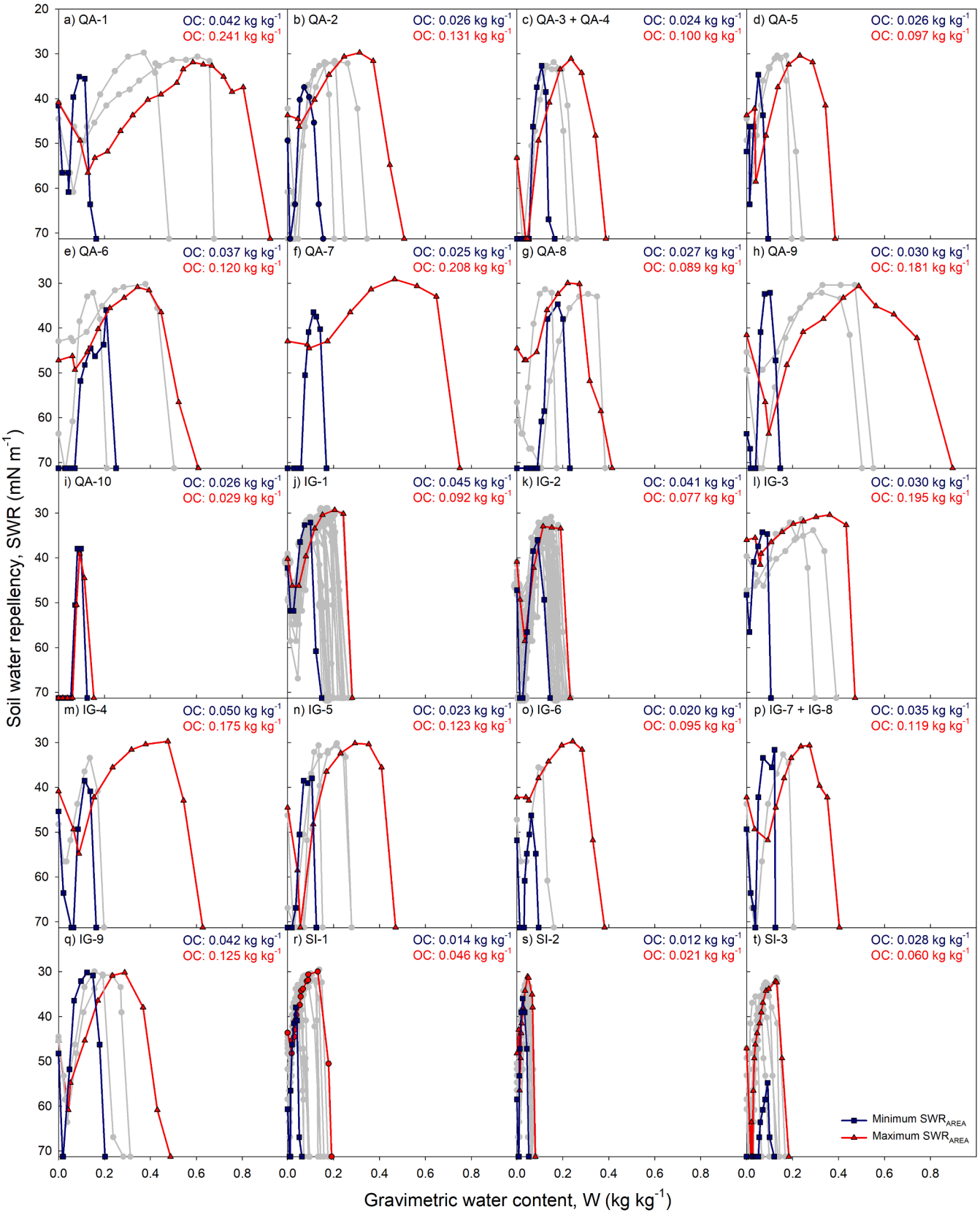

Fig. 4. Soil water repellency versus water content curves for the investigated soil samples collected from 22 fields located in the areas of Qassiarsuk (QA), Igaliku (IG), and Sdr. Igaliku (SI). Blue squares, grey circles, and red triangles, respectively denote the soil samples with the lowest, intermediate, and highest SWR_{AREA} in each plot. The organic carbon content (OC) of the soil samples with the lowest (blue text) and highest SWR_{AREA} (red text) are given within each box. QA-3 & QA-4 as well as IG-7 & IG-8 was merged into two plots for brevity. Note the inverted y-axis, as SWR is inversely related to surface tension.

Table 1
Descriptive statistics of soil properties of 144 hydrophobic soils in this study: organic carbon (OC), clay (<2 μm), silt (2–50 μm), and sand (0.05–2 mm) content, pH, loss-on-ignition (LOI) at 225 °C (LOI_{225}) and 550 °C (LOI_{550}), the SWR_{AREA} and W_{NON}.

Region	Fields	Samples	Stat.	OC kg kg^{-1}	Clay kg kg^{-1}	Silt kg kg^{-1}	Sand kg kg^{-1}	pH –	LOI_{225} kg kg^{-1}	LOI_{550} kg kg^{-1}	SWR^{a}_{AREA} mN m^{-1} kg kg^{-1}	W^{b}_{NON} kg kg^{-1}
QA[c]	10	33	Mean	0.054	0.100	0.303	0.597	5.5	0.136	0.190	9.58	0.355
			Min	0.012	0.040	0.118	0.467	4.5	0.031	0.055	1.43	0.094
			Max	0.154	0.186	0.370	0.821	7.5	0.527	0.609	25.89	0.921
			Std	0.040	0.039	0.061	0.083	0.8	0.120	0.141	7.29	0.220
IG[d]	9	80	Mean	0.048	0.064	0.249	0.686	5.1	0.093	0.141	6.06	0.221
			Min	0.011	0.017	0.052	0.378	4.5	0.028	0.050	1.17	0.095
			Max	0.161	0.194	0.442	0.841	6.1	0.294	0.406	19.42	0.628
			Std	0.021	0.038	0.069	0.098	0.3	0.042	0.055	3.10	0.089
SI[e]	3	31	Mean	0.016	0.032	0.162	0.806	5.6	0.036	0.052	2.70	0.104
			Min	0.005	0.017	0.052	0.699	5.1	0.017	0.026	0.54	0.052
			Max	0.037	0.056	0.249	0.929	6.1	0.078	0.099	6.19	0.192
			Std	0.008	0.011	0.034	0.042	0.3	0.017	0.022	1.50	0.042
All	23	144	Mean	0.061	0.065	0.249	0.686	5.3	0.091	0.133	6.14	0.227
			Min	0.009	0.017	0.052	0.378	4.5	0.017	0.026	0.54	0.052
			Max	0.241	0.194	0.442	0.929	7.5	0.527	0.609	25.89	0.921
			Std	0.041	0.038	0.069	0.098	0.5	0.074	0.092	4.82	0.151

a: The trapezoidal integrated area of the SWR-W curve; b: The critical water content where the soil becomes hydrophilic; c: Qassiarsuk; d: Igaliku; e: South Igaliku.

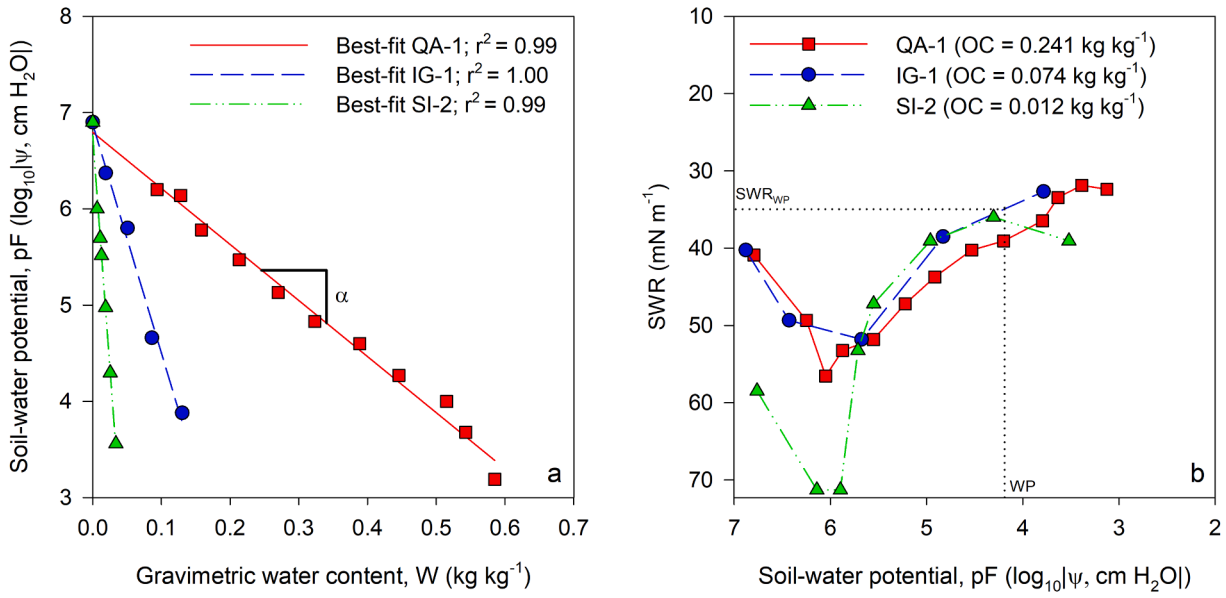

Fig. 5. a) Three representative examples of the fitted soil–water retention curves using the Campbell-Shiozawa (CS) model (Campbell & Shiozawa, 1992). The slope of the CS-model is denoted by α and pF is the common logarithm of the absolute value of the soil–water potential (ψ) in cm H_2O. b) Soil water repellency (SWR) as a function of pF for the same three samples with decreasing organic carbon contents. WP denotes the permanent wilting point (pF = 4.2) and SWR_{WP} represents the interpolated SWR at the permanent wilting point. Note the inverted axes in (b).

is losing mass and changing its quality (Simkovic et al., 2008) caused by thermal degradation and volatilization of organic matter (Wu et al., 2020). We examined how LOI_{225}, as well as the total OM content measured with LOI (LOI_{550}), are linked to SWR parameters. For both SWR_{AREA} and W_{NON}, the linear regressions that included LOI_{225} and LOI_{550} improved the r^2 values compared to those for OC (Fig. 6). For this dataset, LOI_{550} outperformed both OC and LOI_{225} for the determination of SWR_{AREA} and W_{NON}. One explanation for the better performance of LOI_{550} might be that the ratio between LOI_{225} and LOI_{550} increased slightly with increasing OC content (Fig. A2), i.e. LOI_{225}/LOI_{550} increased substantially for soils with OC contents above 0.15 kg kg^{-1}.

3.4. Impacts of texture and clay-to-OC saturation on SWR

The Dexter *n* clay-to-OC ratio had a decreasing effect on both SWR_{105} and SWR_{60} in the Dexter *n* range between 0 and 2 (Fig. 7a and b), and at Dexter n values just above, 2 the SWR_{105} and SWR_{60} ceased. Additionally, SWR_{WP} was negatively correlated with Dexter n (r = -0.39), and SWR_{WP} exhibited a considerable variation from Dexter n values just below 2 and up. (Fig. 7c). The Dexter *n* has also been found to influence SWR in other studies. In the study of Karunarathna et al. (2010b), a Dexter *n* index of 8 was successfully applied to distinguish hydrophilic and hydrophobic soils for a dataset comprised of Japanese soil samples (OC range: 0.6 to 14.1%). The study of de Jonge et al. (2009) calculated the amount of non-complexed OC based on a Dexter *n* index of 10 and found that the SWR_{AREA} exhibited a slightly higher correlation to the amount of non-complexed OC as compared to the total OC. For the present study, non-complexed OC did not exhibit a strong correlation with SWR_{AREA}.

Clay content correlated positively and significantly (P < 0.001) to

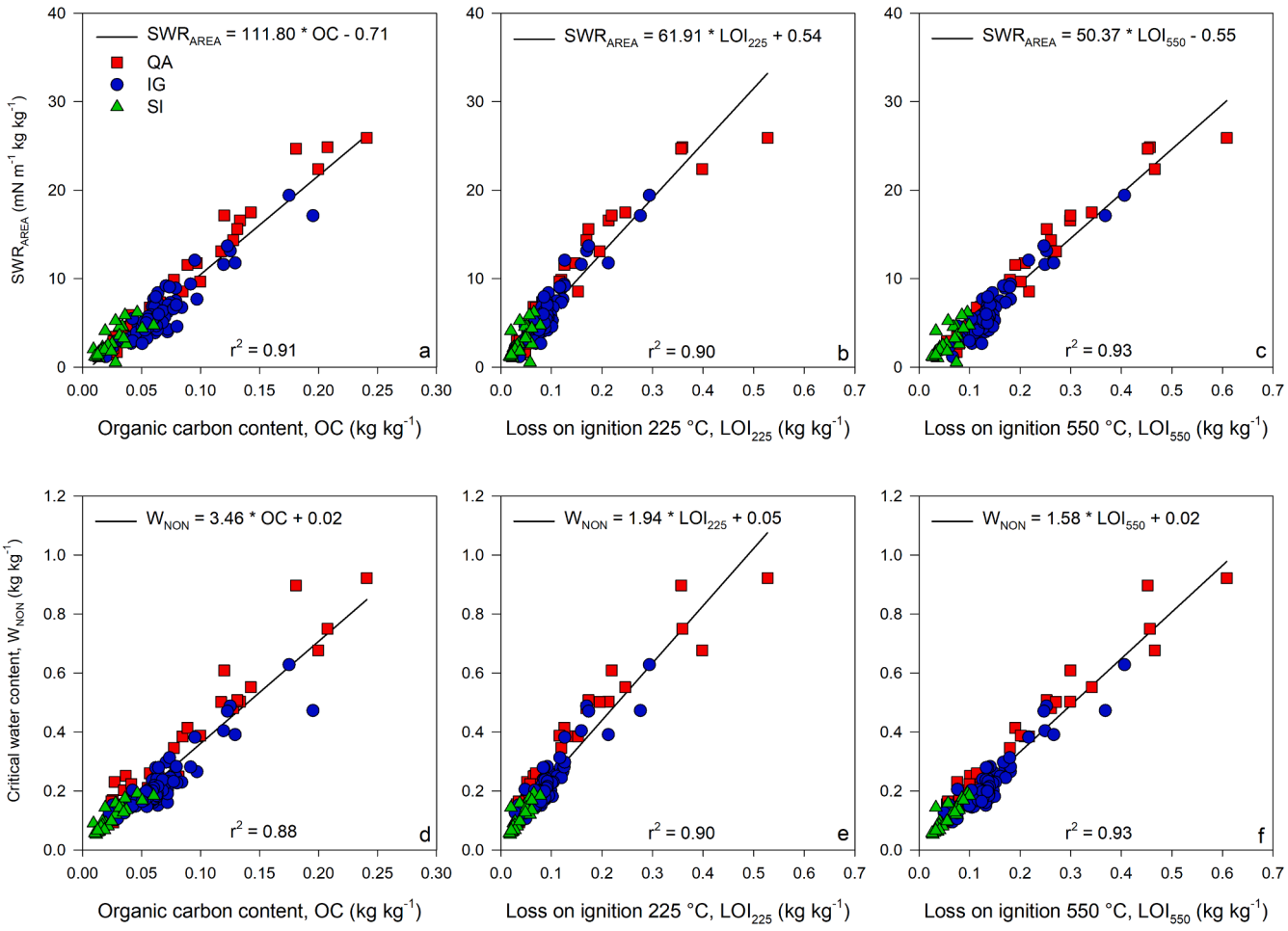

Fig. 6. The integrated trapezoidal area of the SWR-W curve (SWR_{AREA}) as a function of organic carbon content (OC), loss-on-ignition at 225 °C (LOI_{225}), and loss-on-ignition at 550 °C (LOI_{550}) (a–c). The critical soil–water content (W_{NON}) as a function of OC, LOI_{225}, and LOI_{550} (d–f).

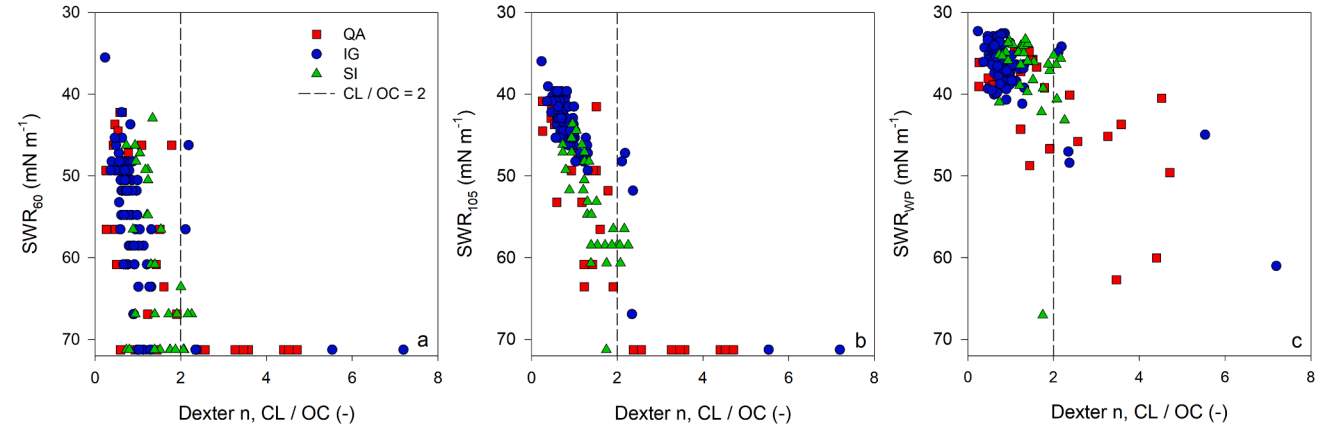

Fig. 7. a) Soil water repellency after the 60 °C pre-treatment (SWR_{60}) as a function of Dexter n (CL/OC), i.e., the ratio of clay content (CL) (kg kg^{-1}) to organic carbon content (OC) (kg kg^{-1}). b) Soil water repellency after the 105 °C pretreatment (SWR_{105}) as a function of Dexter n. c) Soil water repellency at the permanent wilting point, i.e., pF 4.2 (SWR_{WP}) vs Dexter n. The vertical dashed line represent the Dexter n = 2. Note the inverted y-axis, as SWR is inversely related to surface tension.

both SWR_{AREA} and W_{NON} (r = 0.53 and 0.61, respectively; results not shown). Further, clay content significantly improved ($p > 0.001$) the relationship between W_{NON} and both OC and LOI_{550} (Fig. 8) in the forward MLRs. This contrasts the findings of Hermansen et al. (2019), who did not find a significant positive effect of clay content on W_{NON}.

In summary, we identified three effects of texture on the severity of SWR; i) for SWR_{105} and SWR_{60}, the soils became hydrophilic at Dexter *n* values just above 2, ii) SWR_{WP} decreased with increasing Dexter *n*, and iii) clay content improved the predictions of W_{NON} in the MLR including OC and clay content as predictor variables.

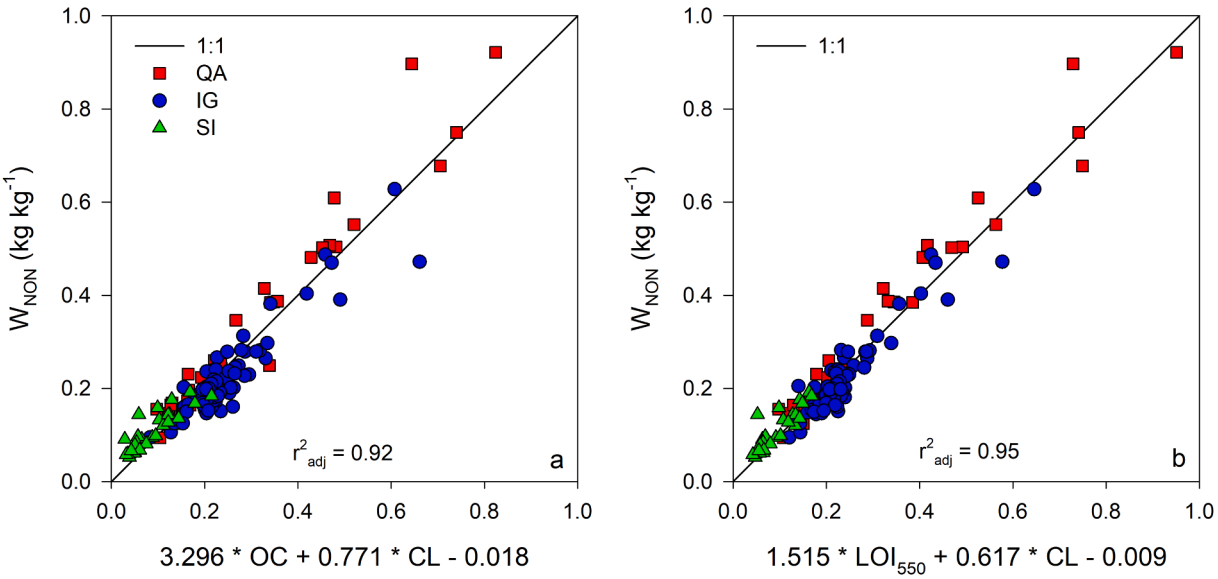

Fig. 8. Best performing multiple linear regressions for the critical soil–water content (W_{NON}) using organic carbon content (OC) (a), and loss-on-ignition at 550 °C (b). CL denotes the clay content, and all parameters are expressed as (kg kg^{-1} dry soil).

3.5. Soil water retention as a predictor of SWR

The link between soil–water retention and SWR was highlighted by the strong linear relationship between $-\alpha^{-1}$ and both SWR_{AREA} (r^2 = 0.87) and W_{NON} (r^2 = 0.93) (Fig. 9). The very strong correlation between W_{NON} and α^{-1} further indicates that the soil water retention dictates the SWR through the pF-dependent orientation of the hydrophobic functional groups and thus W_{NON}. The weaker relationship between SWR_{AREA} and $-\alpha^{-1}$ could be explained by ambiguous clay interactions (shown in Figs. 7 and 8), as clay is likely to decrease the severity in SWR around the wilting point, while simultaneously increasing W_{NON}, and thereby the W range where the soil is hydrophobic. Such an ambiguous clay interaction is also supported by the fact that OC exhibited a weaker correlation to W_{NON} than SWR_{AREA} (Fig. 6). Nevertheless, the results identify $-\alpha^{-1}$ as a promising and novel predictor of both SWR parameters, especially since α^{-1} is relatively easy to determine using a modern dew point potentiometer or vapour sorption analyzer (Arthur et al., 2014; Pittaki-Chrysodonta et al., 2019).

3.6. OC as a controller of SWR across different climatic and geographic regions

We also investigated if the linear relationship between SWR parameters (SWR_{AREA} and W_{NON}) and OC could be extended to other data sets. To this end, we compared the dataset from Greenland with a dataset comprising 72 soil samples from New Zealand (Hermansen et al., 2019). Overall, the range in SWR_{AREA} (0.16–26.85 mN m^{-1}) and W_{NON} (0.07–0.78 kg kg^{-1}) of the New Zealand soil samples was comparable to that of the Greenlandic soil samples.

There were only small deviations between the two datasets in the linear regressions for SWR_{AREA} and W_{NON} (Fig. 10), emphasizing that the effect of OC on the severity in SWR is comparable, even though these samples were collected in different countries under varying climatic conditions.

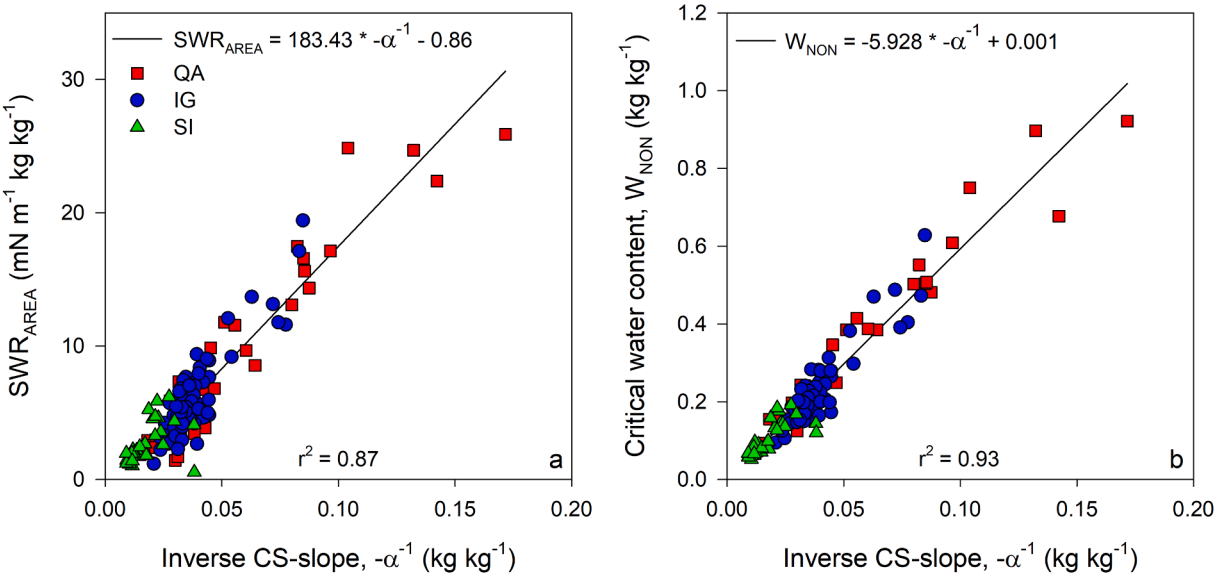

Fig. 9. a) The integrated trapezoidal area of the SWR-W curve (SWR_{AREA}) as a function of the inverse CS-slope, where the inverse CS-slope is the negative reciprocal of the fitted CS-slopes. b) The critical soil–water content (W_{NON}) as a function of the inverse CS-slope.

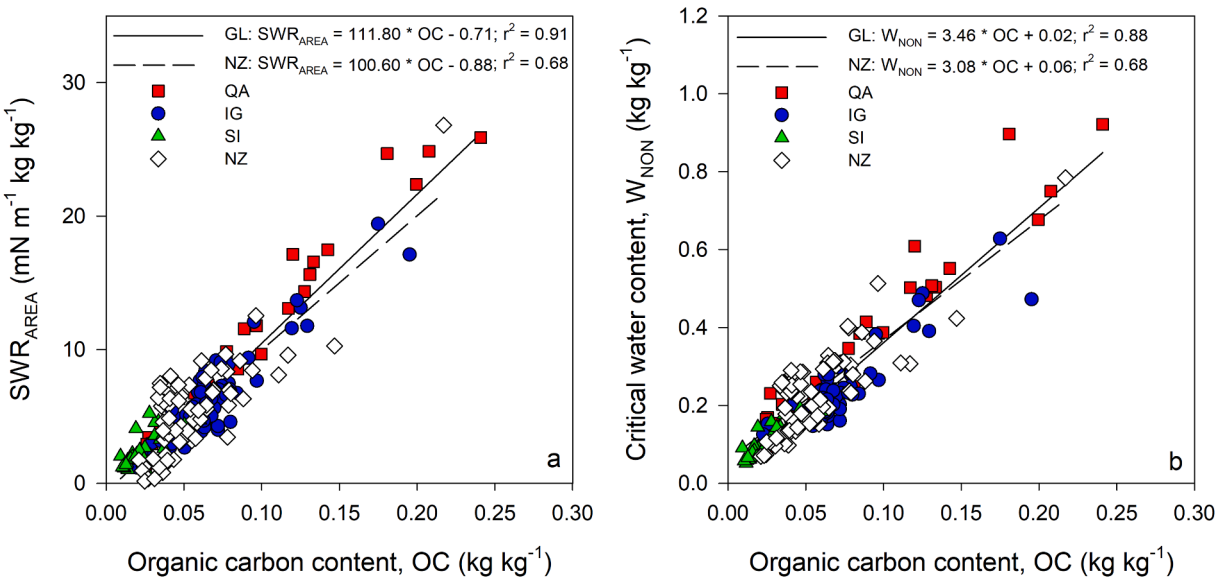

Fig. 10. Comparison of the investigated Greenlandic (GL) soils and 72 New Zealand pasture soils (Hermansen et al., 2019). a) The integrated trapezoidal area under the SWR-W curve (SWR_{AREA}) vs organic carbon content (OC). b) Critical soil–water content (W_{NON}) vs OC.

4. Conclusion

The soils investigated in this study originated from Qassiarsuk, Igaliku and South Igaliku, three of the main agricultural areas in southwest Greenland. Soil water repellency was highly prevalent in the investigated samples, with 99% of the samples exhibiting some degree of SWR and 98% of the soils being extremely hydrophobic at their maximum SWR.

The integrated trapezoidal area under the SWR-W curve (SWR_{AREA}) and the critical water content (W_{NON}) were highly linearly correlated to OC, LOI_{225}, and LOI_{550}. LOI_{550} was identified as the best predictor of these two repellency parameters suggesting the future application of LOI_{550} to assess both the occurrence of SWR and guide irrigation practices in the region.

Interestingly, there were almost identical linear expressions for SWR_{AREA} and W_{NON} based on OC content for the Greenlandic SWR data and samples from New Zealand, which indicates a similar SWR behaviour of these grass and pasture soils from widely different climatic and geographic regions.

Three effects of texture on the SWR-W curves were identified for the Greenlandic soils: SWR_{105} and SWR_{60} decreased with higher Dexter *n* clay-to-OC saturation index, and just above a Dexter *n* ratio of 2, SWR_{105} and SWR_{60} ceased to be hydrophobic. Further, the degree of soil water repellency at the wilting point decreased linearly with increasing Dexter *n*. Lastly, including clay content in the MLRs using OC or LOI_{550} to predict W_{NON} improved the predictions.

There was a strong linear correlation between the inverse of the Campbell-Shiozawa slope ($-\alpha^{-1}$) and both SWR_{AREA} and W_{NON}. Thus, the $-\alpha^{-1}$ can also be used to infer the severity SWR in these sub-arctic soils.

Overall, the strongest pedotransfer functions for SWR_{AREA} and W_{NON} was developed using LOI ($r^2 = 0.93$) and a combination of LOI and clay content ($r^2_{adj} = 0.95$), respectively.

Declaration of Competing Interest

The authors declare that they have no known competing financial interests or personal relationships that could have appeared to influence the work reported in this paper.

Acknowledgments

The authors would like to express their gratitude to the farmers and the Greenlandic Agricultural Consulting Services for their valuable contributions during the fieldwork. Funding: This work was supported by the Danish Council for Independent Research, Technology and Production Sciences via the project: Glacial flour as a new, climate-positive technology for sustainable agriculture in Greenland: NewLand [grant number 022-00184B].

Appendix A. Supplementary data

Supplementary data to this article can be found online at https://doi.org/10.1016/j.geoderma.2021.115189.

References

Arthur, E., Tuller, M., Moldrup, P., Resurreccion, A.C., Meding, M.S., Kawamoto, K., Komatsu, T., de Jonge, L.W., 2013. Soil specific surface area and non-singularity of soil-water retention at low saturations. Soil Sci. Soc. Am. J. 77 (1), 43–53. https://doi.org/10.2136/sssaj2012.0262.

Arthur, E., Tuller, M., Moldrup, P., Wollesen de Jonge, L., 2014. Evaluation of a fully automated analyzer for rapid measurement of water vapor sorption isotherms for applications in soil science. Soil Sci. Soc. Am. J. 78 (3), 754–760. https://doi.org/10.2136/sssaj2013.11.0481n.

Bartoli, F., Regalado, C.M., Basile, A., Buurman, P., Coppola, A., 2007. Physical properties in European volcanic soils: a synthesis and recent developments. In: Arnalds, Ó., Óskarsson, H., Bartoli, F., Buurman, P., Stoops, G., García-Rodeja, E. (Eds.), Soils of volcanic regions in Europe. Springer, Berlin, Heidelberg, pp. 515–537. https://doi.org/10.1007/978-3-540-48711-1_36.

Bisdom, E.B.A., Dekker, L.W., Schoute, J.F.T., 1993. Water repellency of sieve fractions from sandy soils and relationships with organic material and soil structure. Geoderma 56 (1–4), 105–118. https://doi.org/10.1016/0016-7061(93)90103-R.

Campbell, G.S., Shiozawa, S., 1992. Prediction of hydraulic properties of soils using particle-size distribution and bulk density data, in: van Genuchten, M.T. et al. (Eds.), Proceedings of the International workshop on indirect methods of estimating the hydraulic properties of unsaturated soils, Riverside, CA. 11-13 Oct. 1989. US Salinity Lab., Riverside CA. pp. 317-328.

Capriel, P., Beck, T., Borchert, H., Härter, P., 1990. Relationship between soil aliphatic fraction extracted with supercritical hexane, soil microbial biomass, and soil aggregate stability. Soil Sci. Soc. Am. J. 54 (2), 415–420. https://doi.org/10.2136/sssaj1990.03615995005400020020x.

Caviezel, C., Hunziker, M., Kuhn, N., 2017. Bequest of the Norseman—The potential for agricultural intensification and expansion in southern Greenland under climate change. Land 6 (4), 87. https://doi.org/10.3390/land6040087.

Christensen, J.H., Olesen, M., Boberg, F., Stendel, M., Koldtoft, I., 2016. Fremtidige klimaforandringer i Grønland: Kujalleq Kommune, Danish Meteorological Institute, Copenhagen, pp. 1-46. https://www.dmi.dk/fileadmin/user_upload/Bruger_upload/Tema/Klima/15-04-01_kujalleq.pdf (accessed 21 September 2020).

Daanen, R.P., Ingeman-Nielsen, T., Marchenko, S.S., Romanovsky, V.E., Foged, N., Stendel, M., Christensen, J.H., Hornbech Svendsen, K., 2011. Permafrost degradation risk zone assessment using simulation models. Cryosphere 5 (4), 1043–1056. https://doi.org/10.5194/tc-5-1043-2011.

de Jonge, L.W., Jacobsen, O.H., Moldrup, P., 1999. Soil water repellency: effects of water content, temperature, and particle size. Soil Sci. Soc. Am. J. 63 (3), 437–442. https://doi.org/10.2136/sssaj1999.03615995006300030003x.

de Jonge, L.W., Moldrup, P., Jacobsen, O.H., 2007. Soil-water content dependency of water repellency in soils: Effect of crop type, soil management, and physical-chemical parameters. Soil Sci. 172(8), 577-588. doi: 10.1097/Ss.06013e318065c090.

de Jonge, L.W., Moldrup, P., Schjonning, P., 2009. Soil infrastructure, interfaces & translocation processes in inner space ('soil-it-is'): Towards a road map for the constraints and crossroads of soil architecture and biophysical processes. Hydrol. Earth Syst. Sci. 13 (8), 1485–1502. https://doi.org/10.5194/hess-13-1485-2009.

Dekker, L.W., Ritsema, C.J., 1994. How water moves in a water repellent sandy soil.1. Potential and actual water repellency. Water Resour. Res. 30 (9), 2507–2517. https://doi.org/10.1016/S0341-8162(96)00047-1.

Dekker, L.W., Ritsema, C.J., 1995. Fingerlike wetting patterns in two water-repellent loam soils. J. Environ. Qual. 24 (2), 324–333. https://doi.org/10.2134/jeq1995.00472425002400020016x.

Dekker, L.W., Ritsema, C.J., 1996. Variation in water content and wetting patterns in Dutch water repellent peaty clay and clayey peat soils. Catena 28 (1–2), 89–105. https://doi.org/10.1016/S0341-8162(96)00047-1.

Deurer, M., Müller, K., Van den Dijssel, C., Mason, K., Carter, J., Clothier, B.E., 2011. Is soil water repellency a function of soil order and proneness to drought? A survey of soils under pasture in the North Island of New Zealand. Eur. J. Soil Sci. 62 (6), 765–779. https://doi.org/10.1111/j.1365-2389.2011.01392.x.

Dexter, A.R., Richard, G., Arrouays, D., Czyz, E.A., Jolivet, C., Duval, O., 2008. Complexed organic matter controls soil physical properties. Geoderma 144 (3–4), 620–627. https://doi.org/10.1016/j.geoderma.2008.01.022.

Doerr, S.H., Douglas, P., Evans, R.C., Morley, C.P., Mullinger, N.J., Bryant, R., Shakesby, R.A., 2005a. Effects of heating and post-heating equilibration times on soil water repellency. Aust. J. Soil Res. 43, 261–267. https://doi.org/10.1071/SR04092.

Doerr, S.H., Llewellyn, C.T., Douglas, P., Morley, C.P., Mainwaring, K.A., Haskins, C., Johnsey, L., Ritsema, C.J., Stagnitti, F., Allinson, G., Ferreira, A.J.D., Keizer, J.J., Ziogas, A.K., Diamantisf, J., 2005b. Extraction of compounds associated with water repellency in sandy soils of different origin. Aust. J. Soil Res. 43 (3), 225–237. https://doi.org/10.1071/SR04091.

Doerr, S.H., Shakesby, R.A., Walsh, R.P.D., 2000. Soil water repellency: its causes, characteristics and hydro-geomorphological significance. Earth-Sci. Rev. 51 (1–4), 33–65. https://doi.org/10.1016/S0012-8252(00)00011-8.

Francis, J.A., Vavrus, S.J., 2012. Evidence linking Arctic amplification to extreme weather in mid-latitudes. Geophys. Res. Lett. 39 (6), n/a–n/a. https://doi.org/10.1029/2012GL051000.

Gee, G.W., Or, D., 2002. Particle-Size Analysis, in: Dane, J.H., Topp, G.C. Topp (Eds.), Methods of Soil Analysis. Part. 4. Physical Methods. SSSA Book Ser. 5 SSSA, Madison, WI, pp. 255-293.

Giovannini, G., Lucchesi, S., Cervelli, S., 1983. Water-repellent substances and aggregate stability in hydrophobic soil. Soil Sci. 135 (2), 110–113. https://doi.org/10.1097/00010694-198302000-00005.

Graber, E.R., Tagger, S., Wallach, R., 2009. Role of divalent fatty acid salts in soil water repellency. Soil Sci. Soc. Am. J. 73 (2), 541–549. https://doi.org/10.2136/sssaj2008.0131.

Groenevelt, P.H., Grant, C.D., 2004. A new model for the soil-water retention curve that solves the problem of residual water contents. Eur. J. Soil Sci. 55 (3), 479–485. https://doi.org/10.1111/j.1365-2389.2004.00617.x.

Hanna, E., Cappelen, J., 2002. Recent climate of southern Greenland. Weather 57 (9), 320–328. https://doi.org/10.1256/00431650260283497.

Hermansen, C., Moldrup, P., Müller, K., Jensen, P.W., Van den Dijssel, C., Jeyakumar, P., de Jonge, L.W., 2019. Organic carbon content controls the severity of water repellency and the critical moisture level across New Zealand pasture soils. Geoderma 338, 281–290. https://doi.org/10.1016/j.geoderma.2018.12.007.

Hoogsteen, M.J.J., Lantinga, E.A., Bakker, E.J., Groot, J.C.J., Tittonell, P.A., 2015. Estimating soil organic carbon through loss on ignition: effects of ignition conditions and structural water loss. Eur. J. Soil Sci. 66 (2), 320–328. https://doi.org/10.1111/ejss.2015.66.issue-210.1111/ejss.12224.

Jacobsen, N.K., 1987. Studies on soils and potential for soil erosion in the sheep farming area of South Greenland. Arct. Alp. Res. 19 (4), 498–507. https://doi.org/10.2307/1551416.

Karunarathna, A.K., Kawamoto, K., Moldrup, P., de Jonge, L.W., Komatsu, T., 2010a. A simple beta-function model for soil-water repellency as a function of water and organic carbon contents. Soil Sci. 175 (10), 461–468. https://doi.org/10.1097/SS.0b013e3181f55ab6.

Karunarathna, A.K., Moldrup, P., Kawamoto, K., de Jonge, L.W., Komatsu, T., 2010b. Two-region model for soil water repellency as a function of matric potential and water content. Vadose Zone J. 9 (3), 719–730. https://doi.org/10.2136/vzj2009.0124.

Kawamoto, K., Moldrup, P., Komatsu, T., de Jonge, L.W., Oda, M., 2007. Water repellency of aggregate size fractions of a volcanic ash soil. Soil Sci. Soc. Am. J. 71 (6), 1658–1666. https://doi.org/10.2136/sssaj2006.0284.

King, M., Altdorff, D., Li, P., Galagedara, L., Holden, J., Unc, A., 2018. Northward shift of the agricultural climate zone under 21st-century global climate change. Sci. Rep. 8 (1), 7904. https://doi.org/10.1038/s41598-018-26321-8.

King, P.M., 1981. Comparison of methods for measuring severity of water repellence of sandy soils and assessment of some factors that affect its measurement. Aust. J. Soil Res. 19 (3), 275–285. https://doi.org/10.1071/SR9810275.

Leighton-Boyce, G., Doerr, S.H., Shakesby, R.A., Walsh, R.P.D., 2007. Quantifying the impact of soil water repellency on overland flow generation and erosion: a new approach using rainfall simulation and wetting agent on in situ soil. Hydrol. Processes 21 (17), 2337–2345. https://doi.org/10.1002/hyp.6744.

Müller, K., Deurer, M., Slay, M., Aslam, T., Carter, J.A., Clothier, B.E., 2010. Environmental and economic consequences of soil water repellency under pasture. Proc. N. Z. Grassl. Assoc. 72, 207–210. https://doi.org/10.33584/jnzg.2010.72.2786.

Nuttall, M., 2018. Arctic environments and peoples. In: Callan, H. (Ed.), The international encyclopedia of anthropology. John Wiley & Sons Ltd, Hoboken, NJ, pp. 1–7.

Ogrič, M., Knadel, M., Kristiansen, S.M., Peng, Y., De Jonge, L.W., Adhikari, K., Greve, M. H., 2019. Soil organic carbon predictions in Subarctic Greenland by visible–near infrared spectroscopy. Arctic Antarct. Alp. Res. 51 (1), 490–505. https://doi.org/10.1080/15230430.2019.1679939.

Pesch, C., Lamandé, M., de Jonge, L.W., Norgaard, T., Greve, M.H., Moldrup, P., 2020. Compression and rebound characteristics of agricultural sandy pasture soils from South Greenland. Geoderma 380, 114608. https://doi.org/10.1016/j.geoderma.2020.114608.

Pittaki-Chrysodonta, Z., Arthur, E., Moldrup, P., Knadel, M., Norgaard, T., Iversen, B.V., Jonge, L.W., 2019. Comparing visible–near-infrared spectroscopy and a pedotransfer function for predicting the dry region of the soil-water retention curve. Vadose Zone J. 18 (1), 1–13. https://doi.org/10.2136/vzj2018.09.0180.

Pribyl, D.W., 2010. A critical review of the conventional SOC to SOM conversion factor. Geoderma 156 (3), 75–83. https://doi.org/10.1016/j.geoderma.2010.02.003.

Regalado, C.M., Ritter, A., 2005. Characterizing water dependent soil repellency with minimal parameter requirement. Soil Sci. Soc. Am. J. 69 (6), 1955–1966. https://doi.org/10.2136/sssaj2005.0060.

Regalado, C.M., Ritter, A., 2009. A bimodal four-parameter lognormal linear model of soil water repellency persistence. Hydrol. Processes 23 (6), 881–892. https://doi.org/10.1002/hyp.7226.

Regalado, C.M., Ritter, A., de Jonge, L.W., Kawamoto, K., Komatsu, T., Moldrup, P., 2008. Useful soil-water repellency indices: linear correlations. Soil Sci. 173 (11), 747–757. https://doi.org/10.1097/SS.0b013e31818d4163.

Resurreccion, A.C., Moldrup, P., Tuller, M., Ferré, T.P.A., Kawamoto, K., Komatsu, T., de Jonge, L.W., 2011. Relationship between specific surface area and the dry end of the water retention curve for soils with varying clay and organic carbon contents. Water Resour. Res. 47 (6) https://doi.org/10.1029/2010WR010229.

Roy, J.L., McGill, W.B., 2002. Assessing soil water repellency using the molarity of ethanol droplet (MED) test. Soil Sci. 167 (2), 83–97. https://doi.org/10.1097/00010694-200202000-00001.

Schofield, R.K., 1935. The pF of the water in soil, in: Transactions of the third international congress on soil science, vol. 2, July–August 1935. Murby & Co. Oxford, UK, pp. 37–48.

Seaton, F.M., Jones, D.L., Creer, S., George, P.B.L., Smart, S.M., Lebron, I., Barrett, G., Emmett, B.A., Robinson, D.A., 2019. Plant and soil communities are associated with the response of soil water repellency to environmental stress. Sci. Total Environ. 687, 929–938. https://doi.org/10.1016/j.scitotenv.2019.06.052.

Simkovic, I., Dlapa, P., Doerr, S.H., Mataix-Solera, J., Sasinkova, V., 2008. Thermal destruction of soil water repellency and associated changes to soil organic matter as observed by FTIR spectroscopy. Catena 74 (3), 205–211. https://doi.org/10.1016/j.catena.2008.03.003.

Steenfelt, A., Kolb, J., Thrane, K., 2016. Metallogeny of South Greenland: A review of geological evolution, mineral occurrences and geochemical exploration data. Ore Geol. Rev. 77, 194–245. https://doi.org/10.1016/j.oregeorev.2016.02.005.

Weber, P.L., de Jonge, L.W., Greve, M.H., Norgaard, T., Moldrup, P., 2020. Gas diffusion characteristics of agricultural soils from South Greenland. Soil Sci. Soc. Am. J. 1–14 https://doi.org/10.1002/saj2.20114.

Westergaard-Nielsen, A., Bjørnsson, A.B., Jepsen, M.R., Stendel, M., Hansen, B.U., Elberling, B., 2015. Greenlandic sheep farming controlled by vegetation response today and at the end of the 21st century. Sci. Total Environ. 512–513, 672–681. https://doi.org/10.1016/j.scitotenv.2015.01.039.

Wijewardana, N.S., Müller, K., Moldrup, P., Clothier, B., Komatsu, T., Hiradate, S., de Jonge, L.W., Kawamoto, K., 2016. Soil-water repellency characteristic curves for soil profiles with organic carbon gradients. Geoderma 264, 150–159. https://doi.org/10.1016/j.geoderma.2015.10.020.

Wu, Y.C., Zhang, N., Slater, G., Waddington, J.M., de Lannoy, C.F., 2020. Hydrophobicity of peat soils: Characterization of organic compound changes associated with heat-induced water repellency. Sci. Total Environ. 714 https://doi.org/10.1016/j.scitotenv.2019.136444.